Dual Functionalized Graphene Oxide Serves as a Carrier for Delivering Oligohistidine- and Biotin-Tagged Biomolecules into Cells[a]

Batakrishna Jana, Goutam Mondal, Atanu Biswas, Indrani Chakraborty, Abhijit Saha, Prashant Kurkute, Surajit Ghosh*

A versatile method of dual chemical functionalization of graphene oxide (GO) with Tris-[nitrilotris(acetic acid)] (Tris-NTA) and biotin for cellular delivery of oligohistidine- and biotin-tagged biomolecules is reported. Orthogonally functionalized GO surfaces with Tris-NTA and biotin to obtain a dual-functionalized GO (DFGO) are prepared and characterized by various spectroscopic and microscopic techniques. Fluorescence microscopic images reveal that DFGO surfaces are capable of binding oligohistidine-tagged biomolecules/proteins and avidin/biotin-tagged biomolecules/proteins orthogonally. The DFGO nanoparticles are non-cytotoxic in nature and can deliver oligohistidine- and biotin-tagged biomolecules simultaneously into the cell.

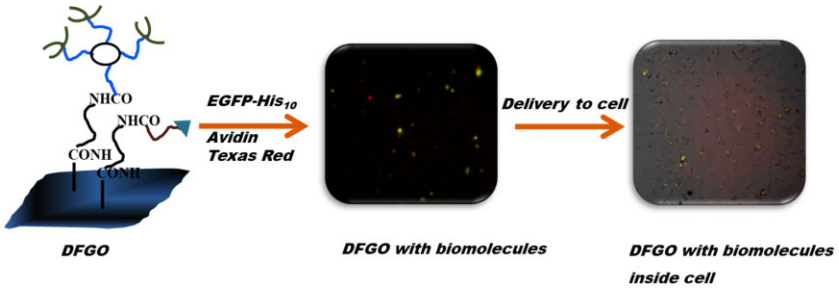

1. Introduction

The structural modification of nano- or micromolecular surfaces by chemical functionalization for the organization of biomolecules has an enormous impact on development of biomedical and biotechnological devices.[1–9] Recently, graphene oxide (GO), a newly emerged two dimensional (2D) one atom thick material has attracted immense interest from large number of scientific communities because of its excellent thermal, mechanical, and electrical properties.[10–14] It has different chemically reactive functionalities, such as epoxy and hydroxyl on the basal plane and carboxylic acid groups along the sheet edge for various functional modifications.[15–17] Several groups have reported the biocompatibility of GO by covalent functionalization of the surface with poly(ethylene glycol)[18–20] as well as further modification of surfaces with proteins,[21–23] nucleic acids,[24–26] drugs, or small molecules[27,28] and subsequent in vitro studies.[26,29–32] Delivery of two different cargo simultaneously into the cell is a challenging task, which requires design and fabrication of dual functionalized delivery vehicles. However, orthogonal functionalization of GO with two different functional groups is not known. Here in, we demonstrate a successful dual covalent functionalization of GO in orthogonal manner and its utility as a novel platform for selective capturing of oligohistidine-tagged protein and biotin- or avidin-conjugated biomolecules for cellular delivery.

B. Jana, Dr. G. Mondal, A. Biswas, I. Chakraborty, A. Saha, P. Kurkute, Dr. S. Ghosh
Chemistry Division, CSIR Indian Institute of Chemical Biology, 4 Raja S. C. Mullick Road, Jadavpur, Kolkata 700032, West Bengal, India
E-mail: sgiicb@gmail.com

[a]**Supporting Information** is available at Wiley Online Library or from the author.

DOI: 10.1002/mabi.201300129

2. Experimental Section

2.1. Synthesis of Dual-Functionalized Graphene Oxide (DFGO)

DFGO was synthesized by following a synthetic scheme as illustrated in Scheme 1. GO, synthesized from graphite powder following a modified Hummer's method,[33,34] was treated with 3 M NaOH followed by ultrasonication for 3 h and neutralized with hydrochloric acid solution to generate carboxy acid functional groups onto GO surface. For subsequent dual functionalization, the carboxy termini of GO was reacted with a 1:1 mixture of diaminopoly(ethylene glycol) (diamino-PEG, H_2N-PEG_{3000}-NH_2) and mono-Boc-amino-PEG ((H_2N-PEG_{3000}-NHBOC) using carbodiimide mediated amide formation reaction. The resultant GO was treated with *N*-hydroxysuccinimide (NHS)-biotin at room temperature for overnight followed by deprotection of *t*-butoxycarbonyl (Boc) group of the other PEG chains using trifluoroacetic acid (TFA). Then, the free amine termini of PEG in the GO was treated with carboxy termini of (O^tBu)Tris-nitrilotris(acetic acid) using carbodiimide mediated amide formation reaction. Finally, the dual-functionalized GO was treated with TFA for the removal of tertiary butyl protection of Tris-nitrilotris(acetic acid) (Tris-NTA). The DFGO nanoparticles form a stable colloidal suspension in BRB 80 buffer upon ultrasonication for 10–15 min followed by probe sonication. The detailed synthetic method is described in the Supporting Information.

3. Results and Discussion

3.1. UV and FT-IR Spectroscopic Analysis

DFGO, labeled with both biotin and Tris-NTA was characterized by UV-Vis and FT-IR spectroscopy. The UV-Vis spectrum of GO recorded in water shows (Figure 1a) the characteristic absorption peaks at 234 and 300 nm. However a similar spectral analysis (Figure 1a) of DFGO shows reduction in intensity of the peak at 234 nm, a significant peak at 300 nm and a new peak at 266 nm (Figure 1a). This indicated covalent functionalizations of GO, and the new peak at 266 nm can presumably be attributed to biotin functionalization (Figure 1a). FT-IR spectral analysis of DFGO (Figure 1b) reveals the presence of a new characteristic peak at 1678 cm^{-1} corresponding to amide carbonyl stretching from the newly formed amide functional groups, which clearly confirmed the proposed covalent functionalization. The significant peaks of DFGO at 1135 and 1511 cm^{-1} are due to C–OH and –C = C– stretching frequencies, respectively. A characteristic peak at 1723 cm^{-1} on the FT-IR spectrum of both GO and DFGO corresponds to the –COOH group of GO and –COOH group of Tris-NTA in DFGO, respectively (Figure 1b).

3.2. Atomic Force Microscopy (AFM)

We analyzed the changes in surface morphology of GO after functionalization by AFM. Both GO and DFGO were deposited on freshly cleaved mica surface independently and dried in air followed by visualization of the surface morphology. AFM images of GO and DFGO reveal that morphology of surface was changed after dual functionalization (Figure 1c,d). The average surface height was found to be increased by a significant level after dual functionalization, as we observed that surface height for GO was 1.21 ± 0.31 nm and that of DFGO was 3.62 ± 1.61 nm (Supporting Information, Figure S1, S2). This result clearly

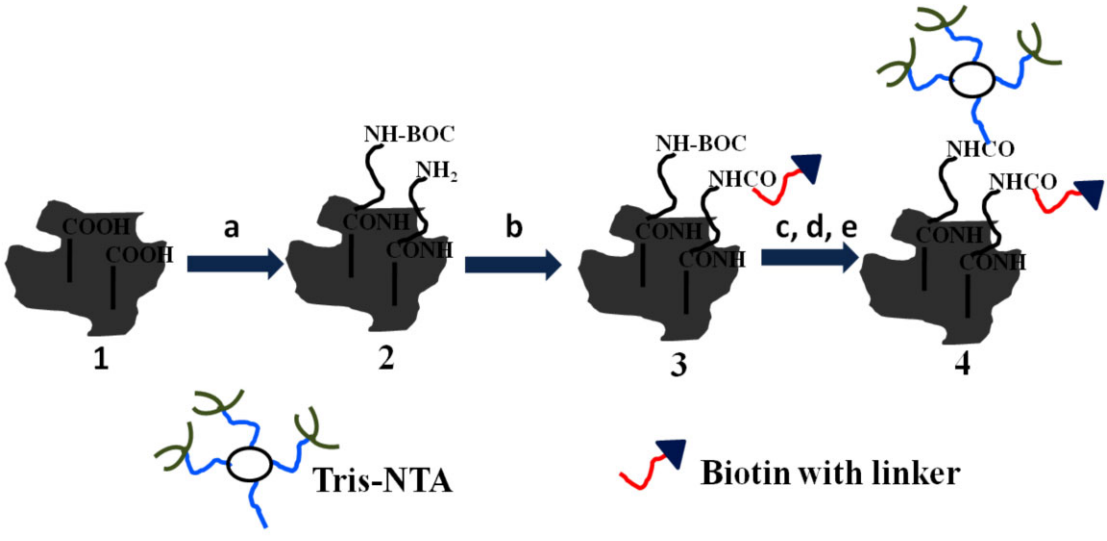

Scheme 1. Synthetic scheme for dual functionalization of GO. a) 1:1 mixture of diaminopoly(ethylene glycol) (H_2N-PEG_{3000}-NH_2) andmono-Boc-amino-PEG(H_2N-PEG_{3000}-NHBOC), N-(3-Dimethylaminopropyl)-N′-ethylcarbodiimide hydrochloride (EDC), β-Mercaptoethanol. b) N-hydroxysuccinimide (NHS)-Biotin, dryN, N′-dimethyl formamide (DMF). c) Trifluoroacetic acid (TFA). d) O-tert butyl protected Tris-[nitrilotris (acetic acid)] [(O^tBu)Tris-NTA] and Diisopropylcarbodiimide (DIC), dry DMF. e) TFA.

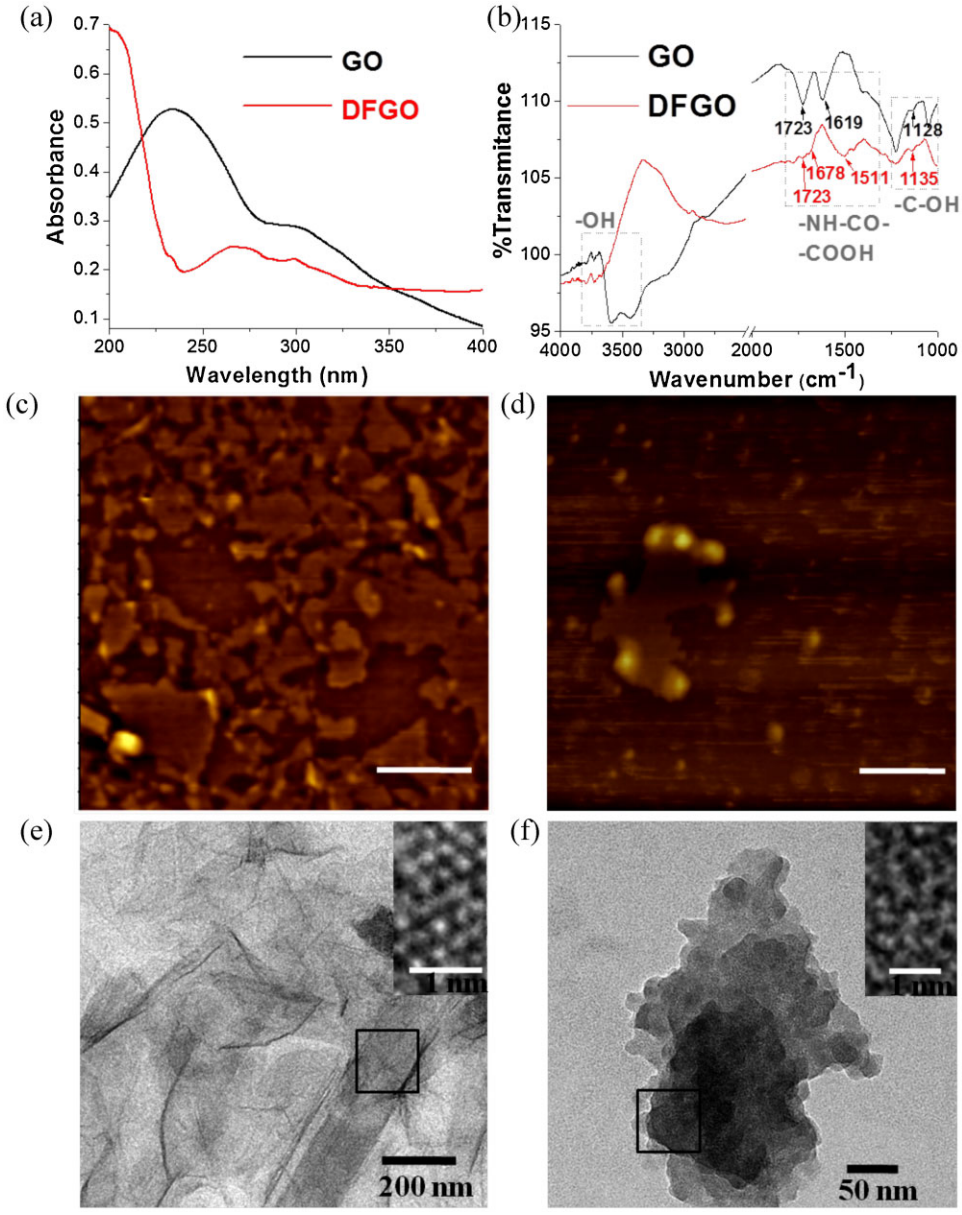

Figure 1. a) UV-Vis spectrum of GO and DFGO; b) IR spectrum of GO and DFGO; c) AFM image demonstrates structure of GO; d) AFM image of DFGO nanoparticles indicating change in morphology (scale bar corresponds to 400 nm); e) HR-TEM image of GO; inset image showing a regular pattern structure of GO surface; f) HR-TEM image of DFGO; inset image represents the absence of this pattern.

confirmed that a more than 2 nm enhancement of average surface height can be attributed to dual functionalization of GO surfaces.

3.3. Transmission Electron Microscopy (TEM) and High-Resolution TEM (HR-TEM) Analysis

Ultra-structural details of GO and DFGO surfaces were characterized by TEM and HR-TEM imaging. We performed TEM and HR-TEM analysis of both GO and DFGO to obtain further details of surface modification in the later. Both GO and DFGO were deposited on carbon coated copper grid independently, dried in air and negatively stained with 2% uranyl acetate solution before imaging under electron microscope. HR-TEM images of GO and DFGO (Figure 1e,f, Supporting Information, Figure S3 and insets) reveal a change in surface morphology after dual functionalization as we observed significant increment of roughness in DFGO in comparison to the GO surface. Further careful analysis revealed that GO surface consists of regular pattern like organized structure, where as in DFGO such a regular pattern is absent.[35] This type of highly resolved

structure clearly shows the structural changes in atomic scale of the GO sheet after covalent functionalization.

3.4. Fluorescence Microscopic Imaging of DFGO After Loading Oligohistidine- and Biotin-tagged Molecules

The structural changes of GO surface after dual functionalization are characterized by various spectroscopic, force microscopic, and HR-TEM. But the question remains whether in reality these covalent functionalization take place for both the functional groups and are they homogeneously functionalized. To address these questions we have checked the biocompatibility and capability of capturing dual fluorophores of the DFGO nanoparticles by fluorescence imaging. It is known that nitrilotris(acetic acid) (NTA) is a very good chelating agent for Ni^{2+} and the Ni^{2+}–NTA complex has been widely used for various types of biochemical and biotechnological applications.[36,37] As a proof of principle, here we have used deca-histidine tagged Enhanced Green Fluorescent Protein (EGFP-His_{10}) recombinant protein to validate Tris-NTA (multivalent head groups containing nitrilotriacetic acid) conjugation and Texas Red Avidin dye to validate biotin conjugation onto DFGO nanoparticles. Briefly, the EGFP-His_{10} and Texas Red Avidin binding ability onto the DFGO nanoparticles were studied as follows. First, DFGO nanoparticles were incubated with Ni^{2+} solution; second, Texas Red Avidin was loaded onto the DFGO nanoparticles and finally EGFP-His_{10} was loaded onto the DFGO nanoparticles, followed by imaging under fluorescence microscope. Fluorescence microscopic images reveal nanometer sized green and red color nanoparticles under 488 and 561 nm laser light (Figure 2a,b and Supporting Information, Figure S4b,c) excitation, respectively. Interestingly, in merge channel it was observed that both the colors were co-localized in case of major number of nanoparticles (Figure 2c and Supporting Information, Figure S4d), which clearly confirms that dual surface functionalization happened in a controlled manner, and the density of both functional groups are homogeneously distributed onto the DFGO nanoparticles. We have further analyzed that whether protein and avidin binding onto the DFGO nanoparticles is a consequence of nonspecific binding or not. For that purpose EGFP-His_{10} and the avidin dye were loaded onto the PEGylated GO in a similar method as described above and analyzed under fluorescence microscope. No signals were observed upon excited by 488 and 561 nm laser (Figure 2d,e), however black colored PEGylated GO particles were observed (Figure 2f) in DIC mode. The control experiment explicitly confirmed that oligo-histidine tagged protein and avidin dye were bound onto the DFGO nanoparticles through dual functionalization in orthogonal way. We also studied the binding ratio of oligo-histidine tagged- to biotin tagged biomolecules on the DFGO surface by changing the ratio of diamino-PEG and mono-Boc-amino-PEG during chemical functionalization and observed the change in fluorescence intensity of EGFP-His_{10} and avidin Texas Red on the DFGO surface. This result indicates that we can qualitatively control the ratio of immobilized biomolecules on DFGO surface by changing the ratio of diamino-PEG and mono-Boc-amino-PEG in the reaction mixture during functionalization (Supporting Information, Figure S5). Detailed method has been described in the Supporting Information.

3.5. Microtubules Binding Onto DFGO Nanoparticles

Biocompatibility of DFGO surfaces was tested by immobilization of functional proteins such as microtubules combined with EGFP-His_{10}. EGFP-His_{10} was immobilized by following the previously described method. Biotinylated and Alexa Fluor-568 labeled taxol stabilized microtubules were prepared and immobilized onto the neutravidin loaded DFGO nanoparticle. Immobilization of microtubules onto the DFGO was observed by confocal microscope. Red microtubules (Figure 2h) were found to be anchored with green DFGO nanoparticles (Figure 2g) and formed a network structure, which was further confirmed by overlay image (Figure 2i). Thus, the DFGO nanoparticles were capable of binding with functional proteins.

3.6. Particle Size Measurement

In addition, the average size of DFGO nanoparticles, loaded with oligohistidine-tagged and avidin-tagged biomolecules was found to be about 482 nm as measured by dynamic light scattering (DLS; Figure 3a).

3.7. Cytotoxicity Test and Cellular Uptake Study

We have further studied whether our DFGO nanoparticles are able to carry oligohistidine- and avidin-tagged biomolecules into cell. To begin with cytotoxicity of the DFGO nanoparticles were checked by the 3-(4,5-dimethylthiazol-2-yl)-2,5-diphenyltetrazolium bromide (MTT) assay[38] and these were found to be non-cytotoxic in nature (Figure 3b). Subsequently, the cellular uptake of oligohistidine- and avidin-tagged biomolecules loaded DFGO nanoparticles was studied using MDA-MB-231 cells. Fluorescence microscopic images reveal an excellent adherence of cells in bright field (Figure 3c). Green (Figure 3d) and red (Figure 3e) nanoparticles were found to be located inside the cells upon excited by 488 and 561 nm laser light, respectively, and co-localization of red and green color in the cells were further observed in overlay image (Figure 3f). The above results clearly indicate that dual biomolecules loaded DFGO nanoparticles has been uptaken by the cell. Further careful analysis of fluorescent images of cellular uptake of dual biomolecules loaded DFGO nanoparticles reveal that EGFP-His_{10} is released from the DFGO surface (Supporting

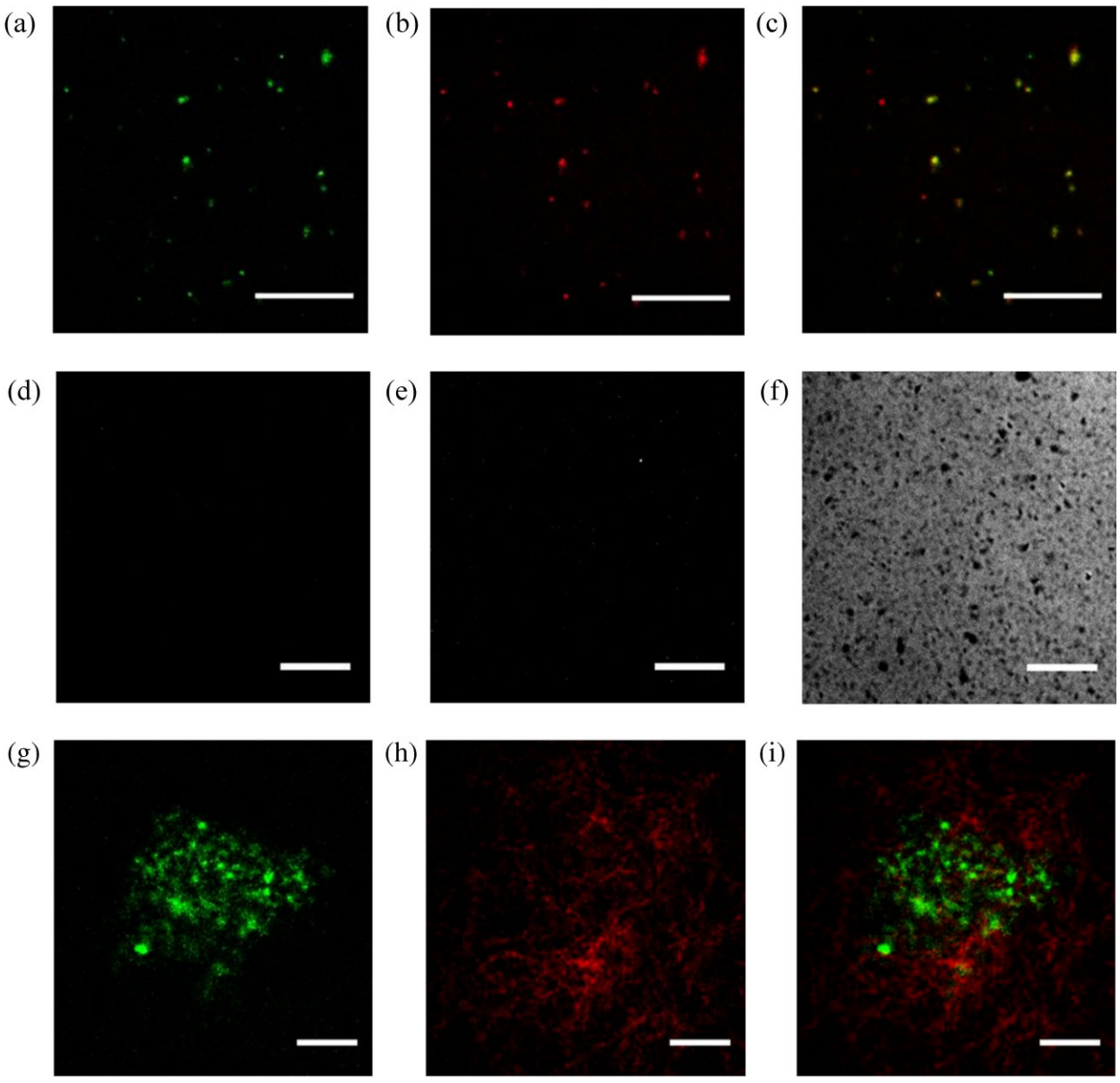

Figure 2. Fluorescence images. a) Green fluorescence of EGFP-His10 and b) red fluorescence of Texas Red Avidin on DFGO nanoparticles was observed under 488 and 561 channel, respectively. c) Yellow merged image of DFGO nanoparticles. d) No green and e) red fluorescence was observed on PEGylated GO nanoparticles under 488 and 561 channel, respectively. f) Black PEGylated GO nanoparticles were observed under DIC mode. g) Green fluorescence from EGFP-His10 bound DFGO nanoparticles through Ni^{2+}–Tris-NTA. h) Red fluorescence from biotin-Alexa568 labeled microtubule network. i) Overlay image indicating microtubules specifically bind on DFGO nanoparticles and form a network structure. Scale bar corresponds to 10 μm.

Information, Figure S6). However, we observed insignificant release of avidin Texas Red dye due to strong biotin/avidin interaction (Supporting Information, Figure S6).

4. Conclusion

In conclusion, we have developed a versatile method of surface functionalization of GO with dual functional groups through covalent chemical functionalization in orthogonal manner. The surface functionalization was thoroughly characterized by various spectroscopic and microscopic imaging techniques. This is a new method of surface modification of GO for selective capturing of functional oligohistidine- and biotin/avidin-tagged various biomolecules/proteins. Moreover, we observed that DFGO nanoparticles are highly biocompatible and non-cytotoxic in nature as proteins/biomolecules

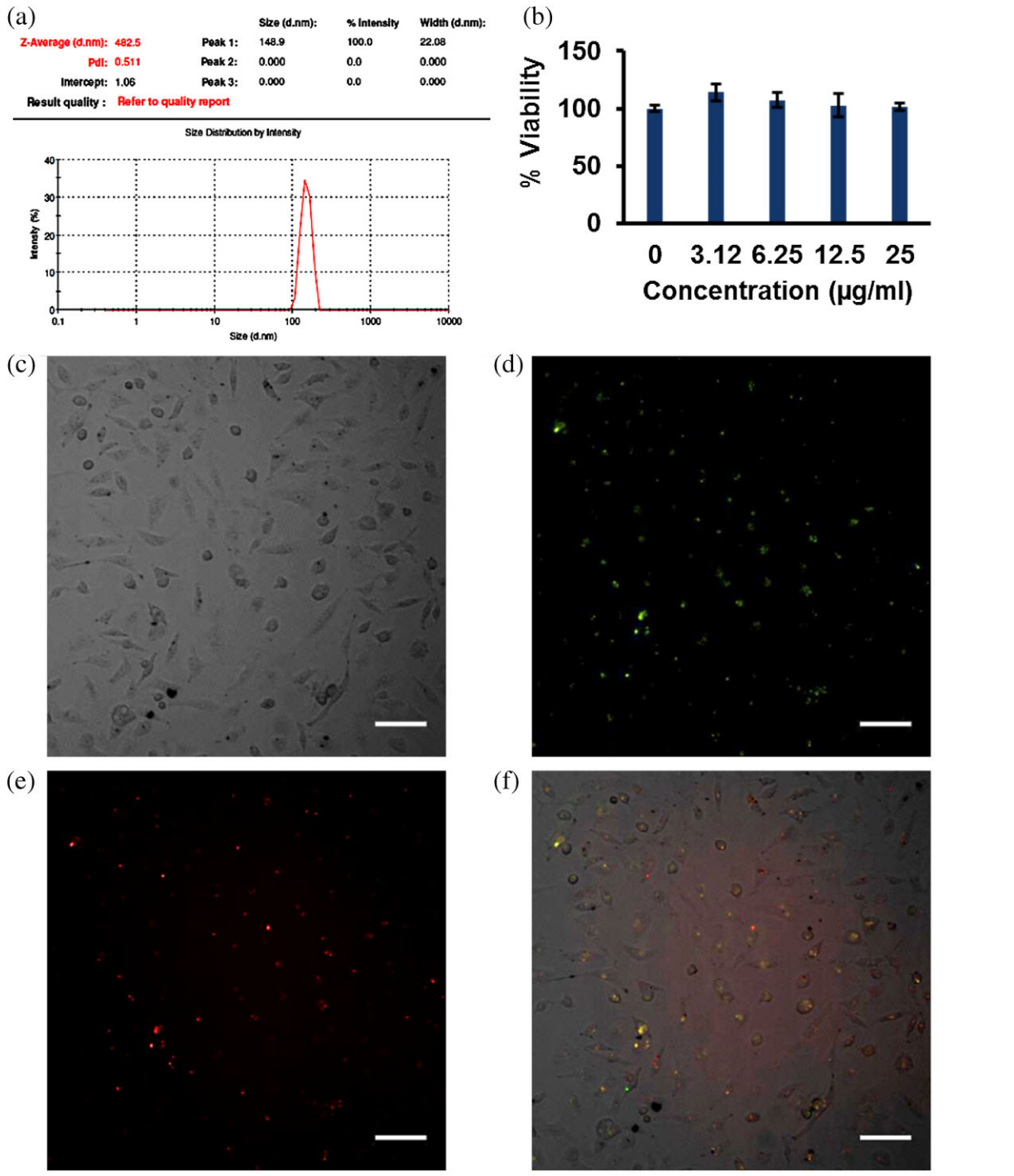

Figure 3. a) DLS was recorded after loading onto DFGO nanoparticles, which clearly indicate that the average particle size is 482 nm. b) Proliferation/survival was assessed by MTT assay, which indicates non-cytotoxic nature of DFGO nanoparticles. EGFP-His10 and Texas Red Avidin loaded DFGO nanoparticles incorporated MDA-MB-231 cells in (c) bright field (d) 488 channel, e) 561 channel. f) Overlay image. Scale bar corresponds to 100 μm.

were captured and delivered into the cell under physiological conditions. This approach introduces ample flexibility of using GO nanoparticles in biological applications as it reduces the danger of protein denaturation. Therefore, DFGO nanoparticles will enable further exploration in various biotechnological applications including target specific drug, therapeutic siRNA, and therapeutic protein delivery.

Acknowledgements: The authors thank D. Sarkar for microscopy, anonymous referees for their comments on how to improve the quality of this manuscript, and T. Muruganandan for AFM. The authors also thank Dr. Nakul C. Maiti and Dr. Ramalingam Natarajan for critically reading the manuscript. B.J., A.S., P.K., and I.C. thank CSIR and A.B. is thankful to UGC, India for their fellowship. S.G. kindly acknowledge to CSIR-IICB and DST, India for the position to work and Ramanujan Fellowship as financial assistance, respectively.

Received: March 5, 2013; Revised: June 3, 2013; Published online: July 23, 2013; DOI: 10.1002/mabi.201300129

Keywords: biotin; cellular delivery; graphene oxide; surface functionalization; Tris-NTA

[1] M. G. van den Heuvel, C. Dekker, *Science* **2007**, *317*, 333.
[2] C. You, M. Bhagawati, A. Brecht, J. Piehler, *Anal. Bioanal. Chem.* **2009**, *393*, 1563.
[3] J. C. Love, L. A. Estroff, J. K. Kriebel, R. G. Nuzzo, G. M. Whitesides, *Chem. Rev.* **2005**, *105*, 1103.
[4] G. Decher, *Science* **1997**, *277*, 1232.
[5] P. Singh, S. Campidelli, S. Giordani, D. Bonifazi, A. Bianco, M. Prato, *Chem. Soc. Rev.* **2009**, *38*, 2214.
[6] P. Singh, G. Lamanna, C. Menard-Moyon, F. Maria Toma, E. Magnano, F. Bondino, M. Prato, S. Verma, A. Bianco, *Angew. Chem. Int. Ed.* **2011**, *50*, 9893.
[7] A. Heckel, D. Seebach, *Angew. Chem. Int. Ed.* **2000**, *39*, 163.
[8] L. Welte, U. García-Couceiro, O. Castillo, D. Olea, C. Polop, A. Guijarro, A. Luque, J. M. Gómez-Rodríguez, J. Gómez-Herrero, F. Zamora, *Adv. Mater.* **2009**, *21*, 2025.
[9] V. López, R. S. Sundaram, C. Gómez-Navarro, D. Olea, M. Burghard, J. Gómez-Herrero, F. Zamora, K. Kern, *Adv. Mater.* **2009**, *21*, 4683.
[10] K. S. Novoselov, A. K. Geim, S. V. Morozov, D. Jiang, Y. Zhang, S. V. Dubonos, I. V. Grigorieva, A. A. Firsov, *Science* **2004**, *306*, 666.
[11] M. Allen, V. Tung, R. Kaner, *Chem. Rev.* **2010**, *110*, 132.
[12] S. Park, R. S. Ruoff, *Nat. Nanotechnol.* **2009**, *4*, 217.
[13] C. N. R. Rao, A. K. Sood, K. S. Subrahmanyam, A. Govindaraj, *Angew. Chem. Int. Ed.* **2009**, *48*, 7752.
[14] Y. X. Xu, H. Bai, G. W. Lu, C. Li, G. Shi, *J. Am. Chem. Soc.* **2008**, *130*, 5856.
[15] A. Lerf, H. He, M. Forster, J. Klinowski, *J. Phys. Chem. B* **1998**, *102*, 4477.
[16] W. Cai, R. D. Piner, F. J. Stadermann, S. Park, M. A. Shaibat, Y. Ishii, D. Yang, A. Velamakanni, S. J. An, M. Stoller, J. An, D. Chen, R. S. Ruoff, *Science* **2008**, *321*, 1815.
[17] S. Stankovich, R. D. Piner, S. T. Nguyen, R. S. Ruoff, *Carbon* **2006**, *44*, 3342.
[18] Y. Liu, D. Yu, C. Zeng, Z. Miao, L. Dai, *Langmuir* **2010**, *26*, 6158.
[19] Z. Liu, J. T. Robinson, X. Sun, H. Dai, *J. Am. Chem. Soc.* **2008**, *130*, 10876.
[20] H. Chen, M. B. Muller, K. J. Gilmore, G. G. Wallace, D. Li, *Adv. Mater.* **2008**, *20*, 3557.
[21] J. H. Jung, D. S. Cheon, F. Liu, K. B. Lee, T. S. Seo, *Angew. Chem. Int. Ed.* **2010**, *49*, 5708.
[22] J. Shen, M. Shi, B. Yan, H. Ma, N. Li, Y. Hu, M. Ye, *Colloids Surf. B* **2010**, *81*, 434.
[23] X. Zuo, S. He, D. Li, C. Peng, Q. Huang, S. Song, C. Fan, *Langmuir* **2010**, *26*, 1936.
[24] C. H. Lu, H. H. Yang, C. L. Zhu, X. Chen, G. N. Chen, *Angew. Chem. Int. Ed.* **2009**, *48*, 4785.
[25] S. He, B. Song, D. Li, C. Zhu, W. Qi, Y. Wen, L. Wang, S. Song, H. Fang, C. Fan, *Adv. Funct. Mater.* **2010**, *20*, 453.
[26] Y. Wang, Z. Li, D. Hu, C. T. Lin, J. Li, Y. Lin, *J. Am. Chem. Soc.* **2010**, *132*, 9274.
[27] X. Sun, Z. Liu, K. Welsher, J. T. Robinson, A. Goodwin, S. Zaric, H. Dai, *Nano Res.* **2008**, *1*, 203.
[28] X. Yang, X. Zhang, Z. Liu, Y. Ma, Y. Huang, Y. Chen, *J. Phys. Chem. C* **2008**, *112*, 17554.
[29] L. Zhang, Z. Lu, Q. Zhao, J. Huang, H. Shen, Z. Zhang, *Small* **2011**, *7*, 460.
[30] Y. Guo, S. Guo, J. Ren, Y. Zhai, S. Dong, E. Wang, *ACS Nano* **2010**, *4*, 5512.
[31] J. M. Englert, C. Dotzer, G. Yang, M. Schmid, C. Papp, J. M. Gottfried, H. P. Steinrück, E. Spiecker, F. Hauke, A. Hirsch, *Nat. Chem.* **2011**, *3*, 279.
[32] J. T. Robinson, S. M. Tabaknam, Y. Liang, H. Wang, H. S. Casalongue, D. Vinh, H. Dai, *J. Am. Chem. Soc.* **2011**, *133*, 6825.
[33] S. Stankovich, D. A. Dikin, G. H. B. Dommett, K. M. Kohlhaas, E. J. Zimney, E. A. Stach, R. D. Piner, S. T. Nguyen, R. S. Ruoff, *Nature* **2006**, *442*, 282.
[34] W. S. Hummers, R. E. Offeman, *J. Am. Chem. Soc.* **1958**, *80*, 1339.
[35] M. H. Gass, U. Bangert, A. L. Bleloch, M. H. Gass, U. Bangert, A. L. Bleloch, *Nat. Nanotechnol.* **2008**, *3*, 676.
[36] S. Lata, M. Gavutis, R. Tampe, J. Pieler, *J. Am. Chem. Soc.* **2006**, *128*, 2365.
[37] Z. Huang, P. Hwang, D. S. Watson, L. Cao, F. C. Szoka, *Bioconjug. Chem.* **2009**, *20*, 1667.
[38] Y. V. Mahidhar, M. Rajesh, A. Chaudhuri, *J. Med. Chem.* **2004**, *47*, 3938.